The principal modes of variability of the boreal winter Hadley cell

Jie Ma[1,2] and Jianping Li[1,3]

Received 31 August 2007; revised 9 November 2007; accepted 4 December 2007; published 12 January 2008.

[1] The year-to-year variability of the boreal winter mass stream function of the mean meridional circulation (MMC) is dominated by an equatorially asymmetric mode and a symmetric mode. The former (latter) mode is linked with the boreal Hadley cell mainly on the decadal (interannual) time-scale. The asymmetric mode index (AMI), which indicates the strength of this mode, shows a clear upward trend during the last decades of the 20th century. The strong sea surface temperature (SST) warming in the tropical Indo-west Pacific warm-pool might be an important factor contributing to the intensification of the asymmetric mode, and the SST warming in the southern tropical Atlantic Ocean and southeast Pacific may also contribute to this intensification. The symmetric mode index (SMI) shows a significant interannual variability that has a very robust and consistent correlation with ENSO, implying that the variability of the Hadley cell is mainly associated with ENSO on the interannual time-scale. Additionally, the symmetric mode variability is also connected with the SST in the tropical Indo-west Pacific warm-pool. **Citation:** Ma, J., and J. Li (2008), The principal modes of variability of the boreal winter Hadley cell, *Geophys. Res. Lett.*, *35*, L01808, doi:10.1029/2007GL031883.

1. Introduction

[2] Many scientists pointed out that the boreal winter (DJF) Hadley cell has been strengthening over the past several decades [*Chen et al.*, 2002; *Quan et al.*, 2004; *Tanaka et al.*, 2004; *Mitas and Clement*, 2005, 2006]. Although the increasing trends are not consistent across all data sets, the trends have been found to be consistent across the NCEP/NCAR and ERA40 reanalysis [*Mitas and Clement*, 2005]. Some studies reported that several factors, such as the tropical heating processes [e.g., *Mitas and Clement*, 2006], ENSO [*Arkin*, 1982; *Oort and Yienger*, 1996], the tropical sea surface temperature (SST) [*Kumar et al.*, 2004; *Hurrell et al.*, 2004], the atmospheric stability [e.g., *Schneider*, 1977], extra-tropical eddy dynamics [*Walker and Schneider*, 2006], and others [e.g., *Lu et al.*, 2007], influence the variability of the Hadley circulation. As for the reason of the enhancing of the Hadley circulation on the decadal time scale, *Quan et al.* [2004] suggested that the warming of the tropical ocean and increased El Niño frequency and amplitude after 1976 contributed to this. However, after removing the ENSO signal from the index of the Hadley circulation the upward trend still exists, and *Mitas and Clement* [2005] therefore indicated that this is in contrast to the partial attribution by *Quan et al.* [2004]. This suggests that the role which ENSO plays in the intensification of the DJF Hadley cell is still an open question. Besides, *Dima and Wallace* [2003] studied the seasonality of the Hadley cell and showed two roughly comparable components of the annual march of the climatological mean meridional circulations (MMCs). However, the principle modes in the year-to-year variability of DJF MMC and their connections with the tropical SST anomalies are not clear at present. In this study we employ EOF analysis to determine the principle modes of year-to-year variability of the DJF Hadley cell and explore their possible connections with the tropical SST anomalies. The NCEP/NCAR reanalysis (1948–2005) [*Kalnay et al.*, 1996] and ERA40 reanalysis (1960–2000) [*Uppala et al.*, 2005] on a 2.5° × 2.5° latitude-longitude grid and NOAA Reynolds SST dataset (1948–2005) [*Smith and Reynolds*, 2004] on a 2.0° latitude × 2.0° longitude grid are used. Following *Oort and Yienger* [1996] the intensity of Hadley cell index (HCI) is defined as the maximum value of the mass stream function [*Wu and Tibaldi*, 1988; *Li*, 2001] of MMC in the latitudinal zone of 0°–30°N. An ENSO index during the same period comes from the website (http://jisao.washington.edu/data_sets/globalsstenso/). It is the average SST anomaly equatorward of 20-degrees latitude (north and south) minus the average SST poleward of 20-degrees and can capture the low-frequency part of the El Niño/Southern Oscillation phenomenon.

2. The Principal Modes

[3] Figure 1 shows the DJF climatological mean of mass stream function of MMC and spatial patterns of the first two EOF modes of its year-to-year variability. As shown in Figure 1a, the northern Hadley cell is dominant and centers at 15°N, which has the maximum value of about 18×10^{10} kg/s and a large latitudinal extent between 10°S–30°N. However, the southern Hadley circulation between roughly 30°S and 10°S centers at 25°S and is weaker even than the austral Ferrel cell. The leading EOF mode (EOF1) accounts for 55% of the total variance of MMC variability, represents a nearly equatorially asymmetric mode (Figure 1b), and over the low latitudes contains a very large meridional cell component across the equator. The second EOF mode (EOF2) explains 10.3% of the total variance and is basically equatorially symmetric with a pair of tropical cells (Figure 1c) in which the southern cell is slightly stronger than its northern counterpart. By means of EOF analysis, the year-to-year variability of the boreal winter mass stream function of MMC could be mainly decomposed

[1]State Key Laboratory of Numerical Modeling for Atmospheric Sciences and Geophysical Fluid Dynamics, Institute of Atmospheric Physics, Chinese Academy of Sciences, Beijing, China.
[2]National Meteorological Center, China Meteorological Administration, Beijing, China.
[3]College of Atmospheric Sciences, Lanzhou University, Lanzhou, China.

0094-8276/08/2007GL031883$05.00

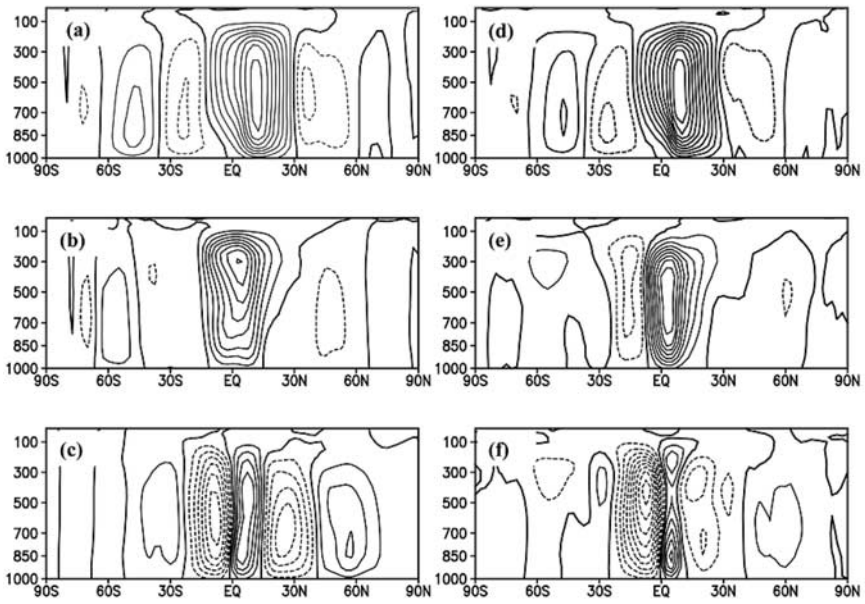

Figure 1. (a) DJF climatology of the mass stream function of MMC from the NCEP/NCAR reanalysis. (b) Leading EOF mode of the DJF MMC (EOF1, accounting for 53.3% of the total variance) from the NCEP/NCAR reanalysis. (c) Second EOF mode of the DJF MMC (EOF2, accounting for 13.3% of the total variance) from the NCEP/NCAR reanalysis. (d) Same as Figure 1a, but for the ERA40 reanalysis. (e) Same as Figure 1b, but for the ERA40 reanalysis. EOF1 accounts for 50.6% of the total variance. (f) Same as Figure 1c, but for the ERA40 reanalysis. EOF2 accounts for 12.7% of the total variance. The period is 1948–2005 for the NCEP/NCAR reanalysis and 1960–2000 for the ERA40 reanalysis. The contour interval is 2×10^{10} kg s^{-1}.

into two principle components: the equatorially asymmetric mode and symmetric mode. These two modes are similar to those in the study of *Dima and Wallace* [2003], but there are distinct differences. The analysis in this study emphasizes the principle modes of year-to-year variability of the DJF winter mass stream function of MMC, whereas that of *Dima and Wallace* [2003] emphasizes the annual march of the climatological MMC. For the sake of convenience, the time series of EOF1 and EOF2 modes of the DJF mass stream function of MMC are defined as the equatorially asymmetric mode index (AMI) and symmetric mode index (SMI), respectively.

[4] Table 1 shows the correlation coefficients among the AMI and SMI of the DJF MMC and the DJF HCI, its 7-yr high-pass (HCI-h) and low-pass (HCI-l) time series. The AMI and SMI are all significantly correlated with the HCI, but the symmetric mode can explain little of the variability of HCI. Further analysis shows that the correlation between the AMI (SMI) and HCI is mainly on the decadal (interannual) time scale (Table 1). These results imply that the equatorially asymmetric mode of MMC is linked with the Hadley cell mainly on the decadal time-scale, and the equatorially symmetric mode is associated with the Hadley cell mainly on the interannual time-scale.

[5] The AMI (Figure 2, top) exhibits a significant upward trend on the decadal time scale, and EOF1 underwent a decadal transform from the negative phase to positive phase at the middle 1970s, suggesting that the variability of the equatorially asymmetric mode of MMC greatly contributes to the enhancing of the northern Hadley cell during the last decades. Figure 2 (bottom) displays that there is no significant trend in the SMI, but evidently interannual variability. In other words, the variability of the equatorially symmetric mode might not substantially contribute to the decadal strengthening of the Hadley cell.

[6] Similar results to those from the NCEP/NCAR reanalysis mentioned above, are found using the ERA40 reanalysis (Figures 1e and 1f), and the correlation coefficients of the DJF HCI, AMI and SMI between the two datasets are respectively 0.83 (not shown), 0.90 and 0.64 (Figures 2c and 2d), which are significant at 0.0001 level. Since the length of the NCEP/NCAR reanalysis is longer than the ERA reanalysis, we mainly employ the former to do further diagnosis although similar results can still be obtained from the latter.

3. Connections With the Tropical SST

[7] Figure 3a illustrates the correlation map between the AMI of the DJF MMC and DJF SST. The predominant

Table 1. Correlation Coefficients Among the Equatorially Asymmetric Mode Index and Symmetric Mode Index of the DJF MMC and the DJF Hadley Cell Index, the 7-Year Highpass and Lowpass HCI[a]

	AMI	SMI
HCI	**0.74** (99.9%)	**0.31** (98%)
HCI-h	0.23	**0.47**
HCI-l	**0.87** (99.9%)	(99.9%) 0.01

[a]AMI is asymmetric mode index, SMI is symmetric mode index, and HCI is Hadley cell index. The HCI-h and HCI-l represent the 7-yr highpass and lowpass HCI respectively which were generated by a Gaussian type of filter. Values in parentheses indicate the confidence level.

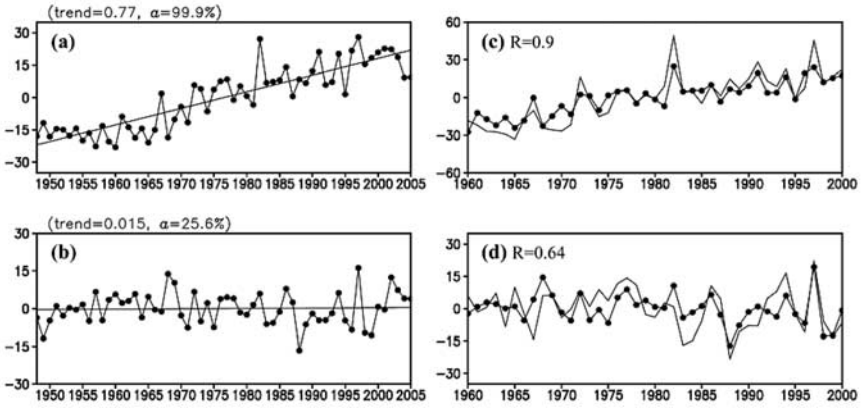

Figure 2. (a) The AMI of the DJF MMC from NCEP/NCAR reanalysis over the period of 1948–2005. (b) Same as Figure 2a, but for the SMI. The linear trend over the whole period and its confidence level are also shown in Figures 2a and 2b. (c) The time series of the AMI, here the closed circle (the real) line getting from the NCEP/NCAR (ERA40) data sets for the period of 1960–2000. (d) Same as Figure 2c, but for SMI. The correlation coefficient between the closed circle and black lines is also shown in Figures 2c and 2d.

correlations between them mostly appear in the low-latitude regions including a large area from the tropical Indian Ocean to the western Pacific warm pool (INWP, 15°S–10°N, 50°E–170°E), the southeast Pacific (SEP, 20°S–5°S, 130°W–70°W) and the southern tropical Atlantic Ocean (STA, 30°S–0°, 40°W–10°E) except the tropical east-middle Pacific (EMP, 5°S–5°N, 160°E–80°W). The correlation map is very similar to the spatial pattern of the linear trend of the DJF SST anomalies (Figure 3c). This suggests that the tropical ocean warming trends in the regions mentioned above are associated with the intensification of the equatorially asymmetric mode of MMC on the decadal time scale. We emphasize that the SST warming in the Indian Ocean-western Pacific warm pool, which could explain 50% variance of the AMI variability (Table 2) and has the strongest trend (Figure 3), might play a dominant role in the decadal strengthening of the Hadley cell. Additionally, the partial contribution from the SST warming in the southeast Pacific and the southern tropical Atlantic Ocean to the decadal strengthening of the Hadley cell can not be ignored (Table 2).

[8] From Figure 3b we can see that the spatial pattern of the significant correlations between the SMI of the DJF MMC and DJF SST robustly appears an ENSO pattern in the EMP region. The robust correlation between the SMI and ENSO is 0.69 (Table 2), while the correlation between the AMI and ENSO is bellow the 95% confidence level, suggesting that the Hadley cell might be associated with ENSO mainly on interannual time scale. Additionally, a broad region of significant correlations between the DJF SMI and SST could also be found in INWP (Figure 3b and Table 2). This implies that the SST in INWP not only plays

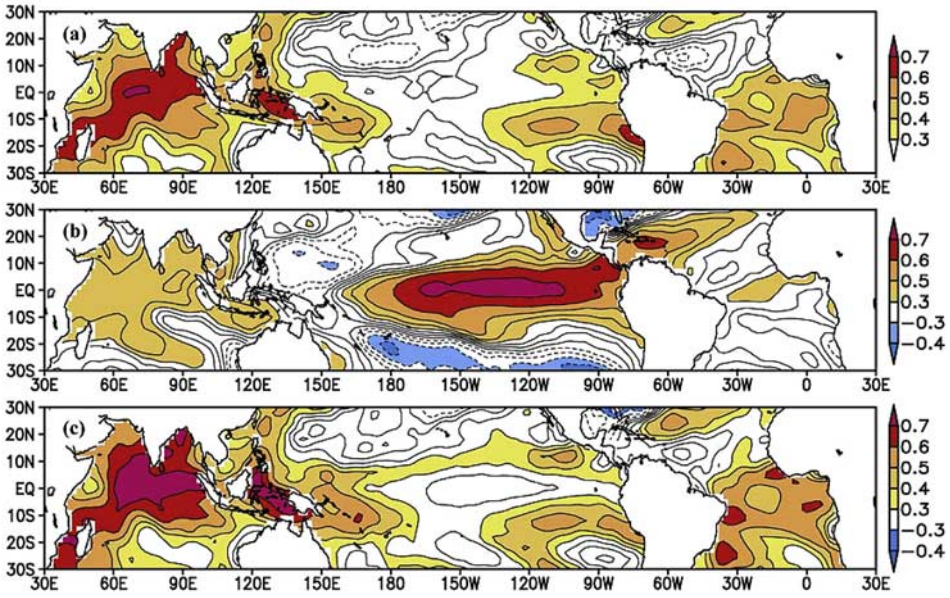

Figure 3. (a) The correlation map between the AMI of the DJF zonal MMC and DJF SST. (b) Same as Figure 3a, but for the SMI. (c) Spatial distribution of the linear trend of the DJF SST. The shaded regions exceed the 98% confidence level.

Table 2. Correlation Coefficients Between Some SST Time Series of INWPI, SEPI, STAI, ENSO, and the AMI and SMI of the MMC for the Boreal Winter[a]

	INWPI	SEPI	STAI	ENSO
AMI	**0.71**	**0.52**	**0.60**	0.24
SMI	**0.33**	**0.40**	0.19	**0.68**

[a]The INWPI, SEPI, and STAI are some SST indices defined as the SST averaged over the areas INWP (15°S–10°N, 50°E–170°E), SEP (20°S–5°S, 130°W–70°W), and STA (30°S–0°, 40°W–10°E), respectively. Values in bold type indicate statistically significant results at the 95% confidence level.

an important role in decadal time-scale variability of the boreal Hadley cell, but also explains certain amount of their covariability on the interannual time scale (that is, the variability of the former is consistent with that of the latter on the interannual time scale).

[9] To further discuss the relationship between ENSO and both the AMI and SMI of the DJF MMC, Figure 4 shows the 15-year moving correlation coefficients between the DJF AMI and ENSO, and the DJF SMI and ENSO. An abrupt change of the moving correlation coefficient between the AMI and ENSO occurs during the middle 1970s, and the correlation coefficients between them are negative before the middle 1970s and positive after that (Figure 4a). Whatever it is before or after 1970s, the moving correlation coefficients between the AMI and ENSO are inconsistent. However, the moving correlations between the SMI and ENSO are consistently significant over the whole period (Figure 4b). These results suggest that removing the ENSO signal from the HCI over the whole period [*Mitas and Clement*, 2005] is equivalent to taking the symmetric mode out from the mass stream function of MMC, therefore even if the ENSO signal is removed from the HCI, the upward trend of the Hadley cell intensity still persists due to strengthening of the asymmetric mode which is associated with the SST warming in INWP, STA and SEP. Besides, these two correlations between the AMI, SMI and ENSO are all positive after 1970s, which may imply the closer connection between the Hadley cell and ENSO during this period and might be a clue to explain why the boreal winter Hadley circulation has been strengthening as El Niño frequency and amplitude after 1976 increased [*Quan et al.*, 2004].

4. Summary and Discussion

[10] The present study investigates the principal modes of the year-to-year variability of the boreal winter Hadley cell, their variability and connections with the tropical SST. Our analysis shows the year-to-year variability of DJF Hadley cell is dominated by an equatorially asymmetric mode and a symmetric mode which are different from the results of the annual march of the climatological MMC by *Dima and Wallace* [2003]. Further analysis also shows that these two modes are closely correlated with the boreal winter Hadley cell on the different time-scale, in detail, the linkage between the Hadley cell and the asymmetric (symmetric) mode is mainly on decadal (inter-annual) time-scale. Moreover, the significant upward trend of the AMI during the last decades implies that the strengthening of the equatorially asymmetric mode, which is linked with the SST warming mainly in the INWP region and partly in the SEP and STA regions, contributes to the enhancing of the Hadley cell. On the other hand, the SMI without any significant trend is consistently and significantly correlated with ENSO, suggesting that the Hadley cell is linked with ENSO mainly on the interannual time scale. The symmetric mode is also consistent with the variability of the SST in the INWP region.

[11] These results might answer the questions raised in the introduction. However, there are still some interesting questions, such as how the strengthening of the AMI corresponds to the SST warming. Otherwise, some researchers pointed out that the Ferrel cell is influenced by the tropical region [*Wang*, 2002a, 2002b] and the annular modes [*Li and Wang*, 2003]. Whether the results of the present study shed some light on the variability of the Ferrel cell and its connection to the upward trend of annular modes of both hemispheres on the decadal time-scale, maybe an interesting future investigation.

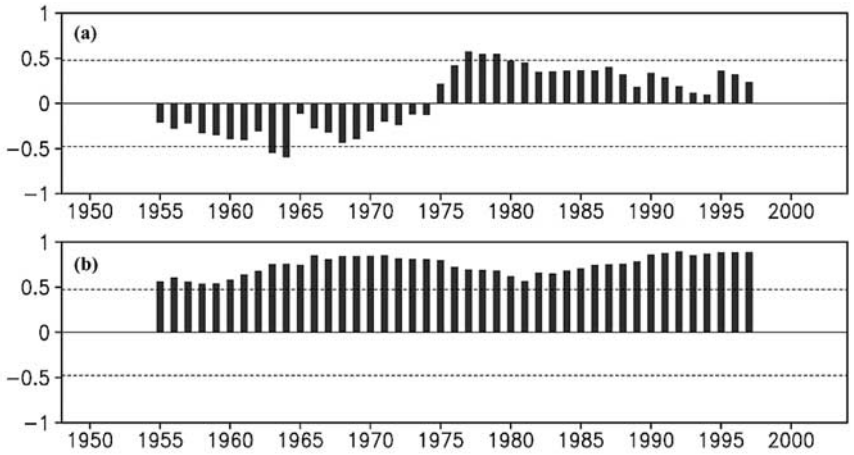

Figure 4. 15-year moving correlation coefficient between (a) DJF AMI and ENSO and (b) the DJF SMI and ENSO. The 95% confidence level is shown by a horizontal dashed line.

[12] **Acknowledgments.** Thanks to two anonymous reviewers for their helpful comments. This work was supported jointly by 973 program (2006CB403600) and NSFC Projects (40528006, 40221503).

References

Arkin, A. (1982), The relationship between interannual variability in the 200 mb tropical wind field and the Southern Oscillation, *Mon. Weather Rev.*, *110*, 1393–1404.

Chen, J. Y., B. E. Carlson, and A. D. Del Genio (2002), Evidence for strengthening of the tropical general circulation in the 1990s, *Science*, *295*(5556), 838–841.

Dima, I. M., and J. M. Wallace (2003), On the seasonality of the Hadley cell, *J. Atmos. Sci.*, *60*, 1522–1527.

Hurrell, J. W., M. P. Hoerling, A. Phillips, and T. Xu (2004), Twentieth century North Atlantic climate change. part I: Assessing determinism, *Clim. Dyn.*, *19*, 371–389.

Kalnay, E., et al. (1996), The NCEP/NCAR 40-year reanalysis project, *Bull. Am. Meteorol. Soc.*, *77*(3), 437–472.

Kumar, A., F. Yang, L. Goddard, and S. Schubert (2004), Differing trends in the tropical surface temperatures and precipitation over land and oceans, *J. Clim.*, *17*, 653–664.

Li, J. (2001), *Atlas of Climate of Global Atmospheric Circulation I. Climatological Mean State*, 279 pp., China Meteorol. Press, Beijing.

Li, J., and J. X. L. Wang (2003), A modified zonal index and its physical sense, *Geophys. Res. Lett.*, *30*(12), 1632, doi:10.1029/2003GL017441.

Lu, J., G. A. Vecchi, and T. Reichler (2007), Expansion of the Hadley cell under global warming, *Geophys. Res. Lett.*, *34*, L06805, doi:10.1029/2006GL028443.

Mitas, C. M., and A. Clement (2005), Has the Hadley cell been strengthening in recent decades?, *Geophys. Res. Lett.*, *32*, L03809, doi:10.1029/2004GL021765.

Mitas, C. M., and A. Clement (2006), Recent behavior of the Hadley cell and tropical thermodynamics in climate models and reanalyses, *Geophys. Res. Lett.*, *33*, L01810, doi:10.1029/2005GL024406.

Quan, X.-W., H. F. Diaz, and M. P. Hoerling (2004), Change in the tropical Hadley cell since 1950, in *The Hadley Circulation: Past, Present, and Future*, edited by H. F. Diaz and R. S. Bradley, pp. 85–120, Cambridge Univ. Press, New York.

Oort, A. H., and J. J. Yienger (1996), Observed interannual variability in the Hadley circulation and its connection to ENSO, *J. Clim.*, *9*, 2751–2767.

Schneider, E. K. (1977), Axially symmetric steady-state models of the basic state for instability and climate studies. part II. Nonlinear calculations, *J. Atmos. Sci.*, *34*, 280–296.

Smith, T. M., and R. W. Reynolds (2004), Improved extended reconstruction of SST (1854–1997), *J. Clim.*, *17*, 2466–2477.

Tanaka, H. L., N. Ishizaki, and A. Kitoh (2004), Trend and interannual variability of Walker, monsoon and Hadley circulations defined by velocity potential in the upper troposphere, *Tellus, Ser. A*, *56*(3), 250–269.

Uppala, S. M., et al. (2005), The ERA-40 re-analysis, *Q. J. R. Meteorol. Soc.*, *612*, 2961–3012.

Walker, C. C., and T. Schneider (2006), Eddy-influences on Hadley circulations: Simulations with an idealized GCM, *J Atmos. Sci.*, *63*(12), 3333–3350.

Wang, C. (2002a), Atmosphere circulation cells associated with the E1 Niño Southern Oscillation, *J. Clim.*, *15*, 399–419.

Wang, C. (2002b), Atlantic climate variability and its associated atmospheric circulation cells, *J. Clim.*, *15*, 1516–1536.

Wu, G. X., and S. Tibaldi (1988), On a computational scheme for atmospheric mean meridional circulation, *Sci. Sin., Ser. B*, *17*(4), 442–450.

J. Li and J. Ma, State Key Laboratory of Numerical Modeling for Atmospheric Sciences and Geophysical Fluid Dynamics, Institute of Atmospheric Physics, Chinese Academy of Sciences, P.O. Box 9804, Beijing 100029, China. (ljp@lasg.iap.ac.cn)